Brazilian Journal of Geophysics, **41** (2023), 1, 49–60
Brazilian Geophysical Society
ISSN 2764-8044
DOI 10.22564/brjg.v41i1.2286

DEFINING COMPOSITIONAL AND TEXTURAL VARIATIONS IN IRON ORES OF THE CAPANEMA MINE, MG, BRAZIL, USING A JOINT INTERPRETATION OF CORE SAMPLES AND GEOPHYSICAL WELL LOGS

Abel Carrasquilla [1*] and Luciano Fonseca [2]

[1]Universidade Estadual do Norte Fluminense Darcy Ribeiro - UENF, LENEP, Macaé, RJ, Brazil
[2]Vale S/A, Mina de Águas Claras (MAC), São Sebastiao das Águas Claras, Nova Lima, MG, Brazil

*Corresponding author: abel@lenep.uenf.br

ABSTRACT. Because density is a fundamental physical characteristic in mineral exploitation, the Brazilian mining company Vale S/A constructed a test site to gather more precise data with the geophysical well log of density. Understanding better the lithological units of three drilling holes at the Capanema Mine, Minas Gerais, Brazil, was the primary goal of this calibration. In the study, geological contacts were compared between those determined by caliper, temperature, natural gamma ray, density, neutron porosity, and sonic wireline logs and those identified by descriptions of core samples. The primary goal of the research was to determine compositional and textural variations in iron formations that were brought on by changes in the rock moisture and hardness. The methodology showed satisfactory results in detecting the presence of clay and hydrated bodies and the transition between friable and compact itabirites. The possibility of altering exploratory drilling meshes with partial replacement of core sampling by rotary percussive boreholes was thus revealed by these results. With this substitution, mineral exploration would be faster and less expensive with the use of well logs to support subsurface geological interpretation.

Keywords: borehole logging, rock samples, iron minerals, compositional variations, textural changes.

INTRODUCTION

Regional geological mapping, aerial geophysical surveys, and subsurface research are part of the industry mineral prospecting process (Kearey et al., 2002). According to this viewpoint, conventional subsurface exploration through drilling wells yields geological medium core samples (CS). Although it offers detailed and localized information, this method is costly and time-consuming (Darling, 2005; Oliveira et al., 2011). Meanwhile, the geophysical well logs (GWL) are helpful, even though they employ indirect measurements, the geophysical well logs (GWL) are helpful (Schön, 2011). Nevertheless, combining the two methodologies can result in more accurate data, taking less time and spending less money (Lüthi, 2001; Rider, 2002). GWL offers several advantages to assist drilling data in defining geological contacts, determining depths, and conducting correlations between wells. However, to complete a job like this, GWL must be adjusted for the effects of drilling mud, mud-cake, invasion, well roughness etc. (Rashidi et al., 2009; Cannon, 2016).

The study area for this project was the Capanema Mine, located in the central location of the Iron Quadrangle, in Minas Gerais State, Brazil (Figure 1). The Itabira Group lithologies, represented by itabirite and hematite rocks of the Cauê Formation (Franco, 2003), are where the mineralization in this mine takes place. The poor thick layer of ore (PLO) that covers these lithologies is known as the Itabira Group (Guimarães et al., 1986). According to Vaz de Melo and Seabra (2000), the structural geology of the area is quite intricate, having been folded by numerous generations of deformational events that duplicated the layers and altered their apparent thickness.

To shorten research time and save expenses, the overall goal of this effort was to enhance iron ore exploration through the integration of CS and GWL

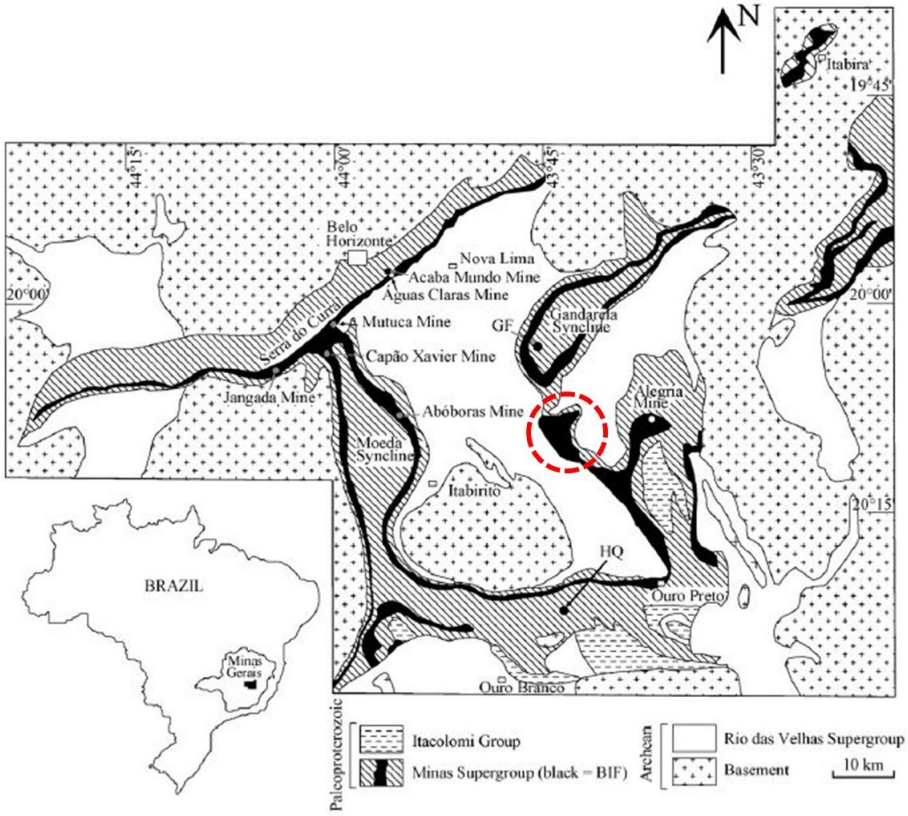

Figure 1: The geographical location of the Iron Quadrangle in Minas Gerais State, highlighting the regional geological outline and the Capanema Mine (dashed red circle). The iron formation units are black, making up the mountains that define the structure: Curral at the north, Moeda, Itabirite at the west, Ouro Preto at the south, and Itabira at the east. The other symbols show more lithological units (Spier et al., 2007).

data. It specifically aimed to find clay horizons, hydrated bodies, the boundary between friable and solid itabirites, the thickness of the weathering layer, and the strata most abundant in iron (Fe).

MATERIALS AND METHODS

The Brazilian Mining Company Vale constructed a test site in a controlled environment (Figure 2) to confidently determine the petrophysical property of the geological formations due to the need for accurate measurements of density log in the ore industry and as part of this study (Instituto de Pesquisas Tecnológicas (IPT), 2011). The Capanema Mine demonstrated key characteristics to develop this work by showcasing features that allow for a systematic and controlled study (Figure 3).

The geological sections of the Capanema Mine are based on the interpretation and chemical analysis of samples from boreholes FD-28, FD-29 and FD-31. This extensive database of the mine aids understanding the regional context (Figure 4). With this knowledge, data were integrated to evaluate significant GWL changes in response to CS compositional and textural changes. The caliper (CAL), temperature (TEMP), natural gamma ray (GR), density (RHOB), neutron porosity (NPHI) and sonic velocity (V_p) wireline logs were utilized in the study. It is crucial to make it clear that the NPHI log has "pu" (porosity units) or "snu" (signal neutral units) units in the figures presented in the article. The highest counts in the variation of the NPHI log in the "snu" unit denote lower hydrogen concentrations and, as a result, lower porosities. The variation in the mineralogical composition may be exhibiting intervals with a higher percentage of hydrated minerals or the presence of water in the rock porosity may be reflected in this circumstance.. The logs were collected by the Weatherford Company in open holes of this mine (Pena, 2013). Subsequently, the softwares WellCad (2014) and MATLAB (2014) were used to process, plot and make the interpretation of the logs.

RESULTS AND DISCUSSIONS

For the three wells, the chemical laboratory analysis of CS roughly reveals Fe percentages of 40% and 60% up to 80.0 m (Figure 5A). On the other hand, the content of silica (SiO_2) increases with a depth of over 30.0% (Figure 5B), and the concentration of alumina (Al_2O_3) decreases to less than 2.0% bellow 40.0m in wells FD-28 and FD-31 (Figure 5C). Therefore, all geological sections have a consistent pattern, with higher clay levels at the top of the boreholes and lower clay levels below 20.0 m. This material, classified as a modified ferruginous rock from 3.6 to 76.9 meters in depth, is known

(A)

(B)

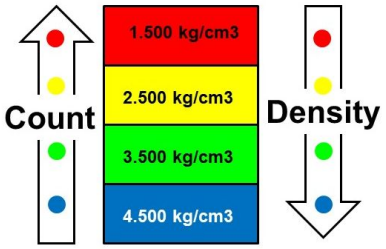

(C)

BLOCK	DENSITY (kg/cm³)	COMPOSITION
1	1.500	Sand, cement + water + styrofoam
2	2.500	1 type of iron ore+ crushed stone + cement + water
3	3.500	3 types of iron ores + crushed stone + cement + water
4	4.500	3 types of iron ores + cement + water

Figure 2: A) Tower in the test site to measure density log. B) Block positioning into the tower with a central hole where GWL tools descend. C) Provision of the blocks with respective density, composition, and counting (IPT, 2011).

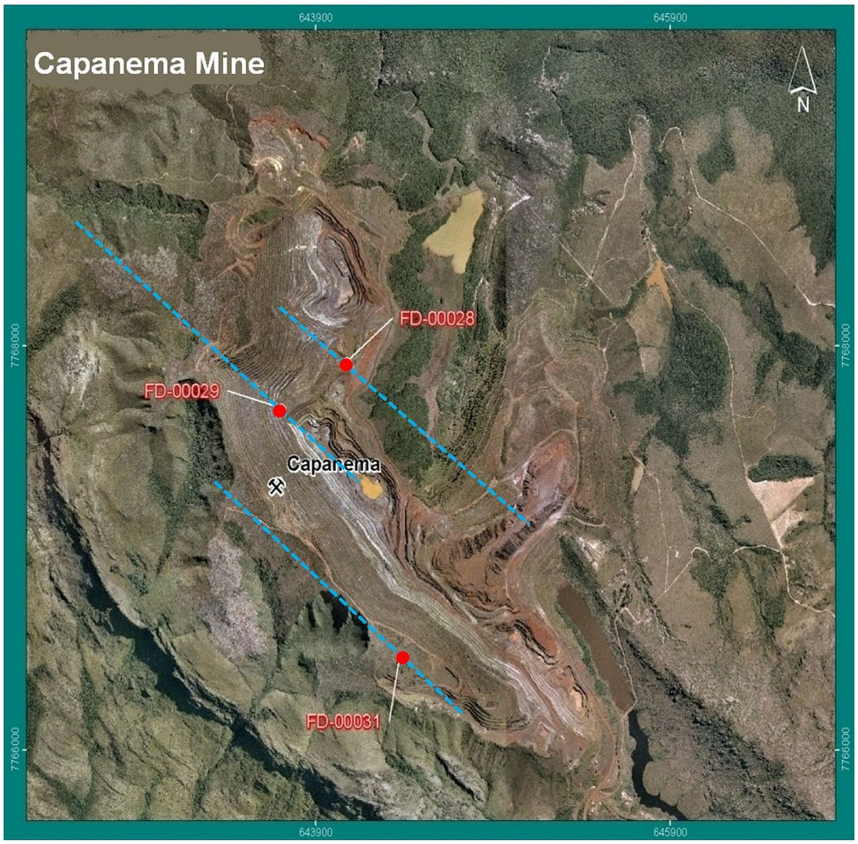

Figure 3: Location of boreholes FD28, FD29 and FD31 in the Capanema Mine. Dashed lines in blue indicate the position of the geological sections (Fonseca, 2014).

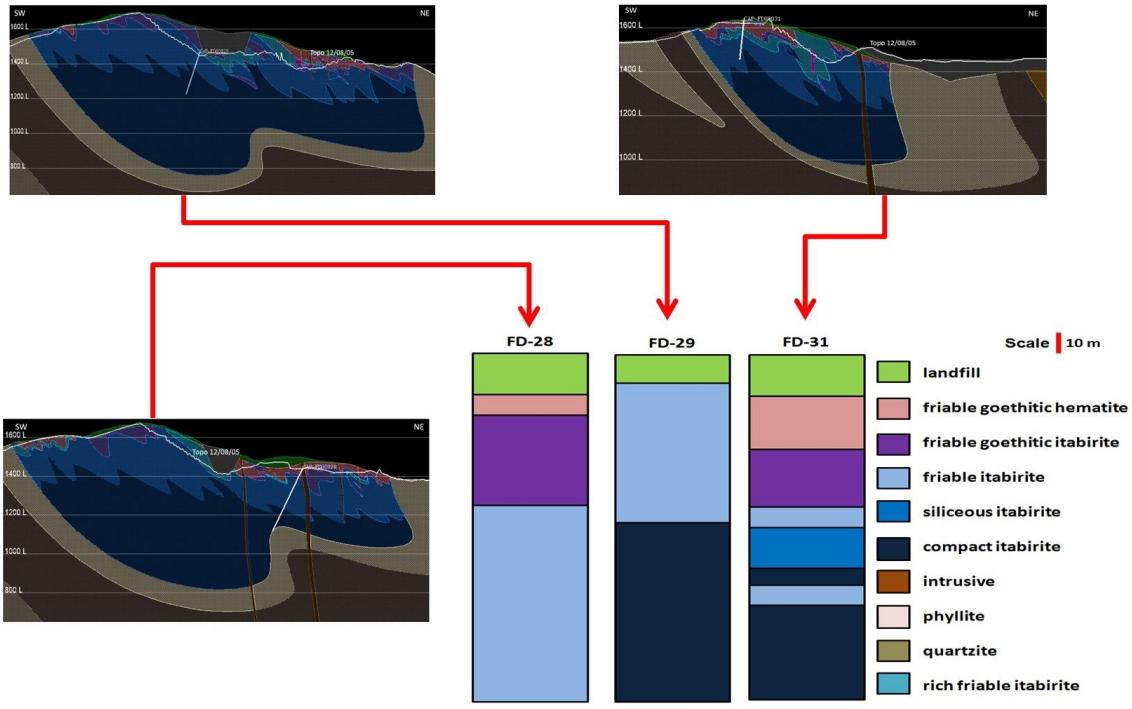

Figure 4: Interpreted geological sections for boreholes FD-28, FD-29 and FD-31. The position of each borehole is highlighted in white in the section (Fonseca, 2014).

as weathered hematite in the area. It is a goethite or hydrated hematite with high iron content (60% Fe; Figure 5A), low SiO_2 (Figure 5B), elevated levels of contaminants like Al_2O_3 (Figure 5C), phosphorus (Figure 5D), and high values of loss on ignition (PF) because of the abundance of hydrated minerals (Figure 5E; Fonseca, 2014).

In each well, the particle size analysis showed a coarser material below 100.0 m deep (Fig. 6A), with a thinner material close to the surface (Figures 6B, C and D). In these figures, the classification of G1 to G4 values indicates the percentage of materials retained in different sieve size classifications, where G1>8.00 mm, 1.00<G2<8.00 mm, 0.15<G3<1.00 mm and G4<0.15 mm (Fonseca, 2014). For well FD-29, Figure 7, prepared from Figure 6A, shows a linear increase of particle size with depth described for the equation G1=1.3 x Depth-8.7, different from the linear relationship G1=Depth, also shown in this figure. Moreover, this figure also shows, respectively, green, yellow, and blue circles for three physical horizons of this well classified as friable (IF), semi-compact (IS), and compact (IC) itabirites. The grouping analysis k-means, which aims to partition n observations into k clusters, drew these circles, wherein each observation belongs to the aggregate with the nearest mean (MATLAB, 2014).

Borehole FD-28 reached a maximum depth of 360.0 m, whose geological description shows a shallow landfill of 20.0 m, passing for goethite hematite up to 21.0 m, followed by an ocher sericite phyllite up to 37.0 and a friable goethite itabirite up to 77.0 m. From there, it goes to the end of the borehole composed of friable itabirites with diverse levels of compactness and progressively lower levels of iron (Figure 4). The logs GR, RHOB, TEMP and CAL recorded the first 98.0 m of this borehole (Figure 8 shows only the first 40.0 m). The GR log shows low range values that indicate a reduction in the presence of clay up to 27.0 m, with the material increasing up to 33.0 m (dashed red rectangle in Figure 8). In Figure 9, at a depth of 51.0 m, the average value of the measured RHOB changes from 3.0 g/cm3 to 3.5 and 4.0 g/cm3, which can be explained by the iron content increase between 47.0 and 77.0 m, particularly in the range that starts at 56.3 m, which assumes a peak concentration (red arrow in Figure 9, which shows only the depth between 48 to 56 m). The CAL log also shows a reduction in the borehole diameter below 51.0 m, showing a transition to a more consistent material (blue arrow in Figure 9, which shows only the depth between 48 to 56 m). However, from 77.0 m, a considerable reduction in the contents of Fe is noticed without declines in RHOB values, decreasing the porosity caused by increased compression (not shown in this work). Although it is noticeable in chemical analysis and geological description, the transition from weathered material to siliceous itabirite is not evident in the logs. The GR log suggests the presence of clays in itabirites throughout the logged interval, supported by the results of the chemical analysis with alumina results above 1.5%, within a depth up to 107.0 m, which is the main kaolinite clay mineral.

Borehole FD-29 reached a depth of 252.9 m, whose geological description indicated a landfill until 12.0 m, getting a friable itabirite below this and evolving to a compact itabirite at 60.0 m (Figure 4). Throughout the hole, itabirites proved to be slightly hydrated with variations in particle size and compactness, initially brittle

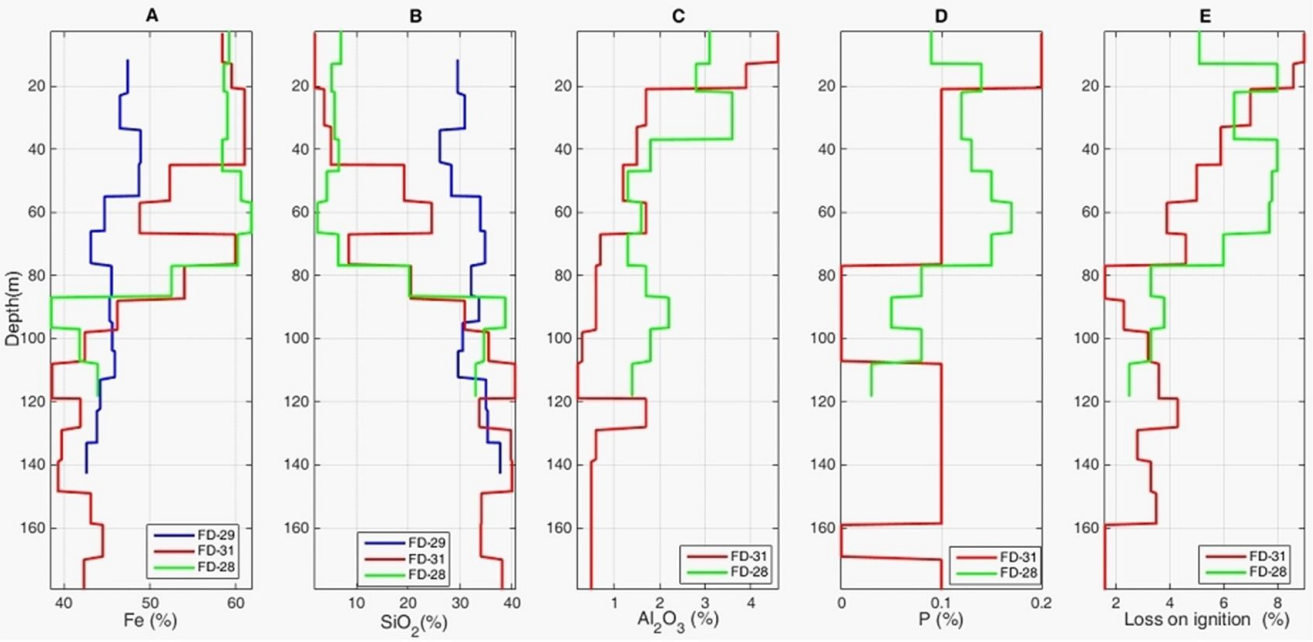

Figure 5: Chemical analysis of samples from wells FD-28, FD-29, and FD-31: (A) Fe, (B) SiO_2, (C) Al_2O_3, (D) P, and (E) loss on ignition (Fonseca, 2014).

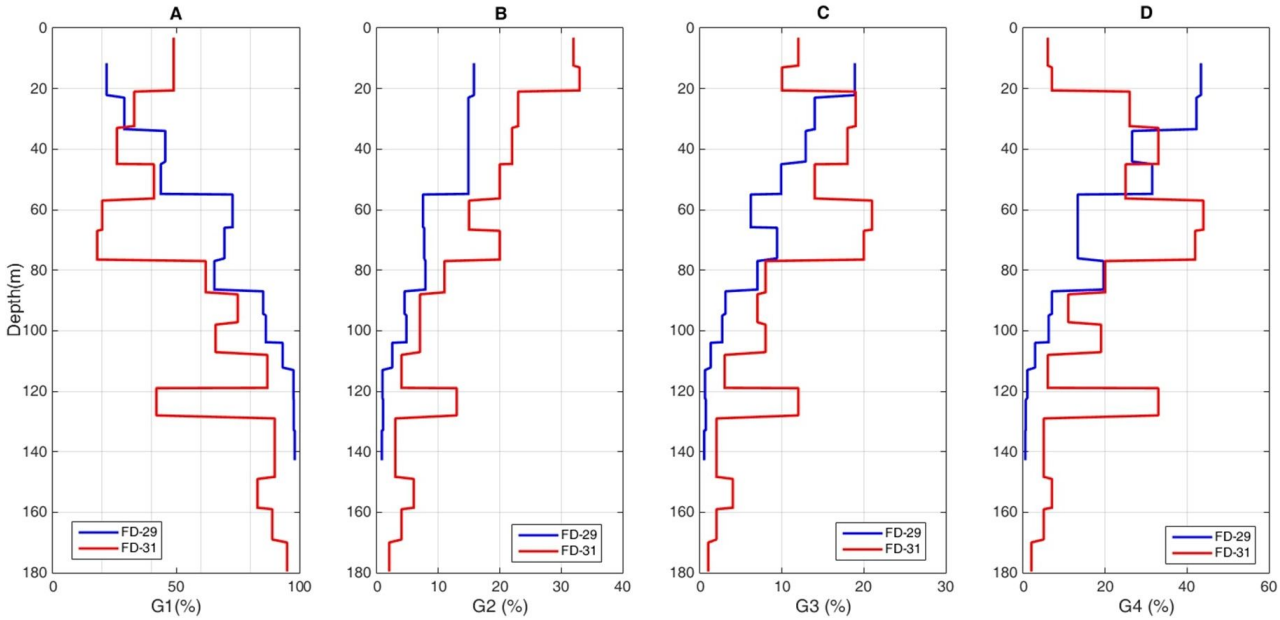

Figure 6: Particle size analysis in wells FD-29 and FD-31 with (A) G1>8.00 mm; (B) 1.00<G2<8.00 mm; (C) 0.15<G3<1.00 mm and (D) G4<0.15 mm (Fonseca, 2014).

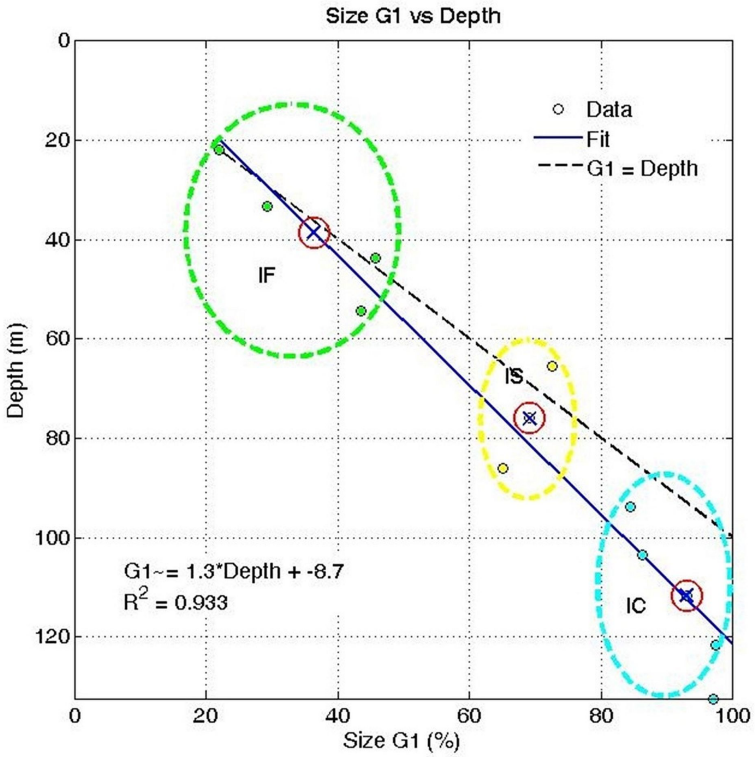

Figure 7: Graph of particle size of the dispersion curve of the thick interval (G1) in borehole FD-29 versus depth, indicating increased compaction with depth and showing the subdivision in groups of friable (IF), semi-compact (IS) and compact (IC) itabirites (Fonseca, 2014).

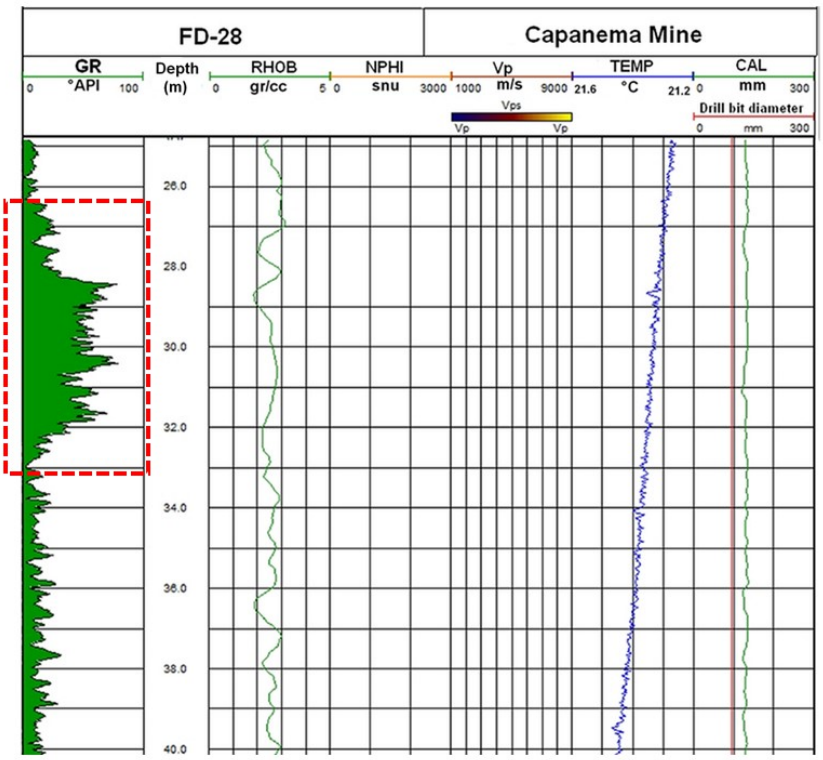

Figure 8: GR log registering the mafic intrusive at a depth between 27.0 and 33.0 m in borehole FD-28. The RHOB, TEMP and CAL logs are also shown on the subsequent tracks (Fonseca, 2014).

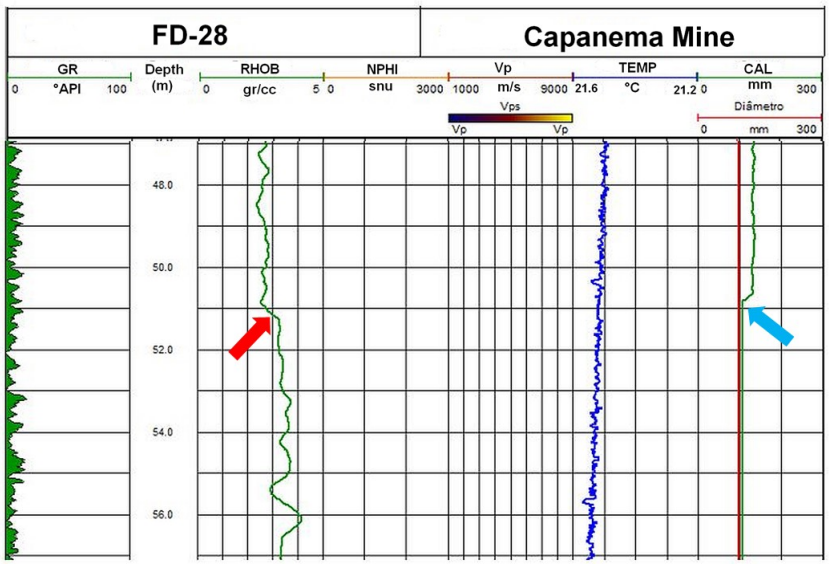

Figure 9: Log details in FD-28 borehole. GR, RHOB, NPHI, V_p, TEMP and CAL logs shown from left to right. The arrows show changes in the RHOB (red) and CAL (blue) logs at 51.0m (Fonseca, 2014).

compact with clay intercalations (left side of Figure 10). It is possible to see a difference of around 4.0 m between the core sample and the log because the range at approximately 6.0 m describes a sericite phyllite zone, representing an altered mafic rock intrusion. The measurement of the GR, RHOB, NPHI, Vp, TEMP and CAL logs got to 133.0 m in this wellbore. On the right side of Figure 10, the GR log shows a sharp drop in the shaliness around 10.0 m, coincident with the more rectilinear pattern of the RHOB curve, which can reflect the contact between the landfill and itabirite. In B, the GR log shows a shaly peak, which coincides with collapses in the borehole, showing a larger diameter measured by the CAL log in C. In D, the decrease in NPHI coincides with a drop point in the RHOB log and a high concentration of clay in the landfill, as shown by the GR log. On the other hand, the CS of this hole is depicted on the left of Figure 11 at depths ranging from 19.0 to 28.30 m, displaying an increase in compression in itabirite ore at a depth of 26.0 m, making the CS more cylindrical. Details of the GR log are shown to the right of this figure, followed by the NPHI and RHOB logs. The RHOB increased to a depth of 26.0 m (Figure 11; dashed red arrow and blue circle) and the NPHI log showed a corresponding decline in porosity. Figure 12 displays the final lithological description alongside the details of the GR, RHOB, NPHI, Vp, TEMP and CAL logs, from left to right. The RHOB log increases, and the NPHI and CAL logs decrease at 63.0 m depth (Break 1). A new NPHI fall and increased RHOB logs occur at 75.0 meters (Break 2). The water table changes the RHOB logs around 85.0 m below this, and also picks up the TEMP log, as shown by the inverted delta.

The V_p log, on the other hand, reaches a low value of 2000.0 m/sec when it reaches 80.0 m, increasing the acoustic wave transit time. All of this behavior was explained as a zone of itabirites transitioning from friable to semi-compact to compact below 75.0 m (Figure 12), with varying degrees of compression. Below 100.0 m, RHOB, NPHI and V_p log details show an increase in density, a decrease in porosity, an increase in compression and a subsequent increase in the V_p, likely due to a rise in the concentration of iron minerals (Figure 13). As a result, the B level exhibits a transition zone-like pattern of little NPHI growth, decreased RHOB, increased compression and increasing V_p log. In the presence of hematite horizons with high iron content, for example, the compression/porosity factor was more important than the rock chemical composition, which differed from the situation in another borehole under study (Fonseca, 2014).

Only 70.0 m of the logs were measured in the borehole FD-31, but with the existence of CS. It passed through a landfill up to a depth of 12.0 m, and from this point up to a depth of 18.9 m; PLO was discovered with only tone variations (left side of Figure 14). Around 22.3 meters down, a red clayey PLO changed into a sandy yellow goethite hematite. From this point, the composition gradually changed to friable goethite hematite at 45.0 m, then to friable goethite itabirite at 76.5 m, which gradually changed to a compact siliceous itabirite. Since all the sections up to this depth are shallow and weathered, goethite, kaolinite and gypsum are abundant and typically found in hydrated environments (Figure 4). The laboratory analysis supported this interpretation, which shows high concentrations of Fe, SiO2 and Al2O3 at this depth (Figure 5). A decrease in Fe and an increase in SiO2 contents, both goethite, can also be used to identify the hematite to itabirite transition (Figure 5). The variations in the RHOB and CAL logs up to 12.0 m of well FD-31 show the shallow landfill, interpreted as the change from a sandy to a clayey horizon of the PLO (right of Figure 14). The presence of clays likely due to mineralogical modifications causes a decrease in the RHOB and an increase in the CAL logs. Still, there is also a decrease in porosity and an increase in density

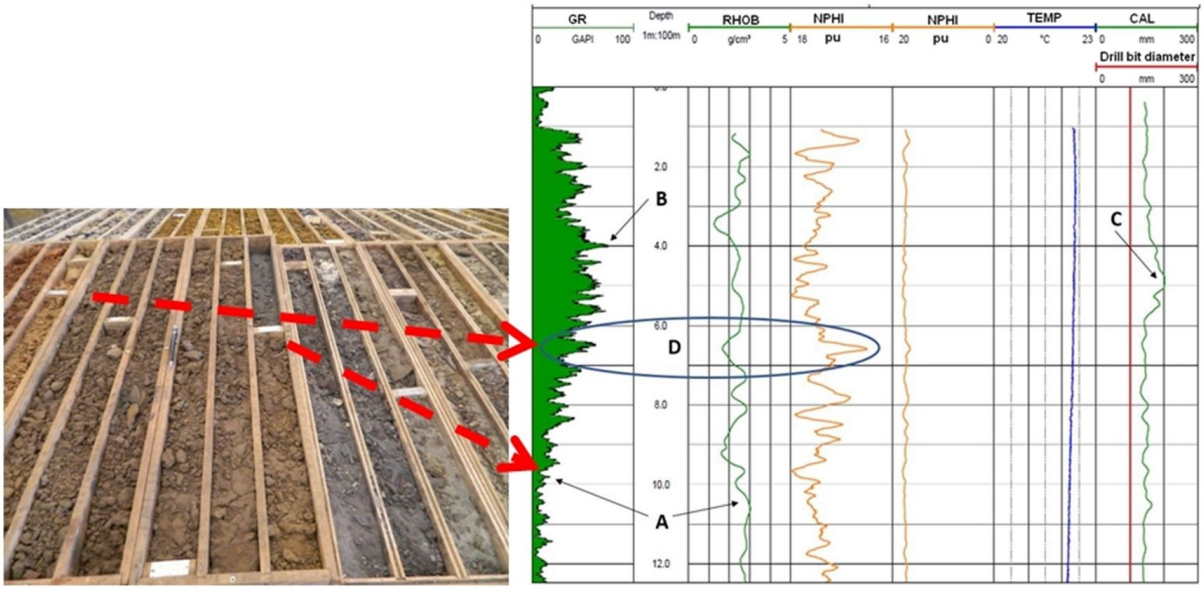

Figure 10: Details on the logs of borehole FD-29: (A) sharp fall in shaliness at 10.0 m, coinciding with the most rectilinear pattern of the RHOB log, reflecting the contact landfill-itabirite; (B) peak of shaliness coincident with the collapse in the borehole walls registered on the CAL log in (C); (D) decrease in porosity recorded in the NPHI log, coinciding with a drop in density (RHOB log) and increased concentration of clay in the landfill (GR log) (Fonseca, 2014).

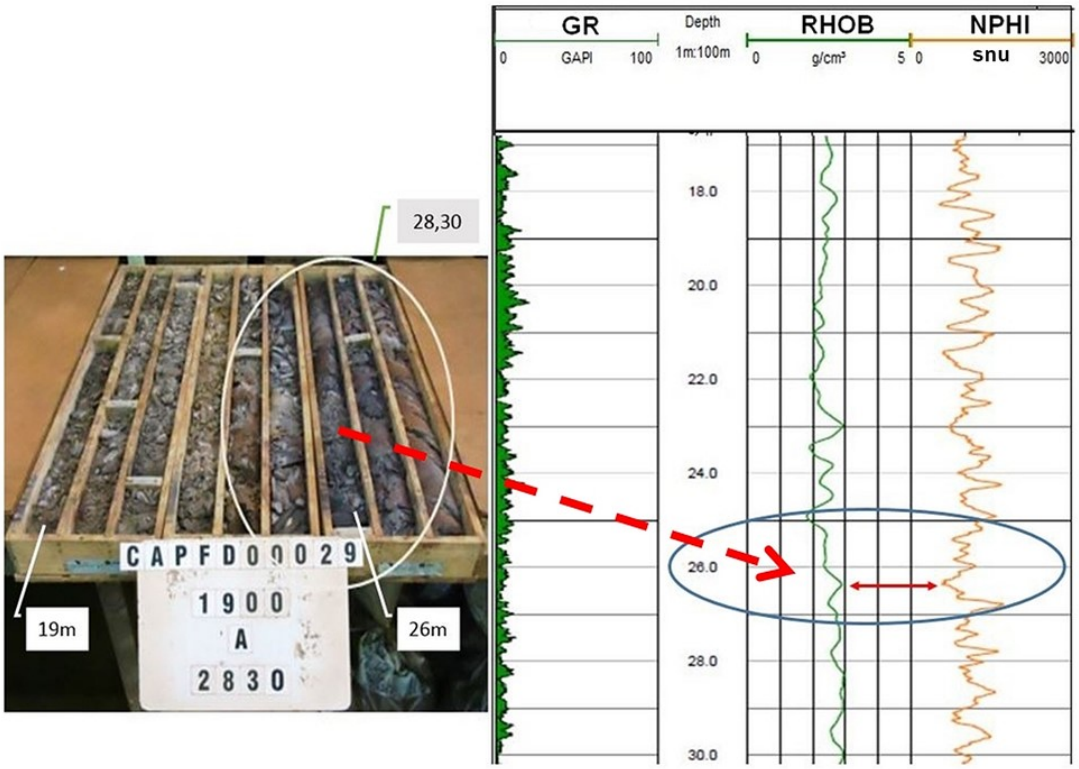

Figure 11: At the left, drill core for the borehole FD-29 between 19.0 and 28.3 m depth, showing increased compactness of the itabiritite ore at around 26.0 m, with cores proving to be more cylindrical. The right part of the figure shows the GR, RHOB and NPHI logs, where it is observed an increase in the density level slightly above 26.0 m depth correlated with a decrease in the NPHI log (Fonseca, 2014).

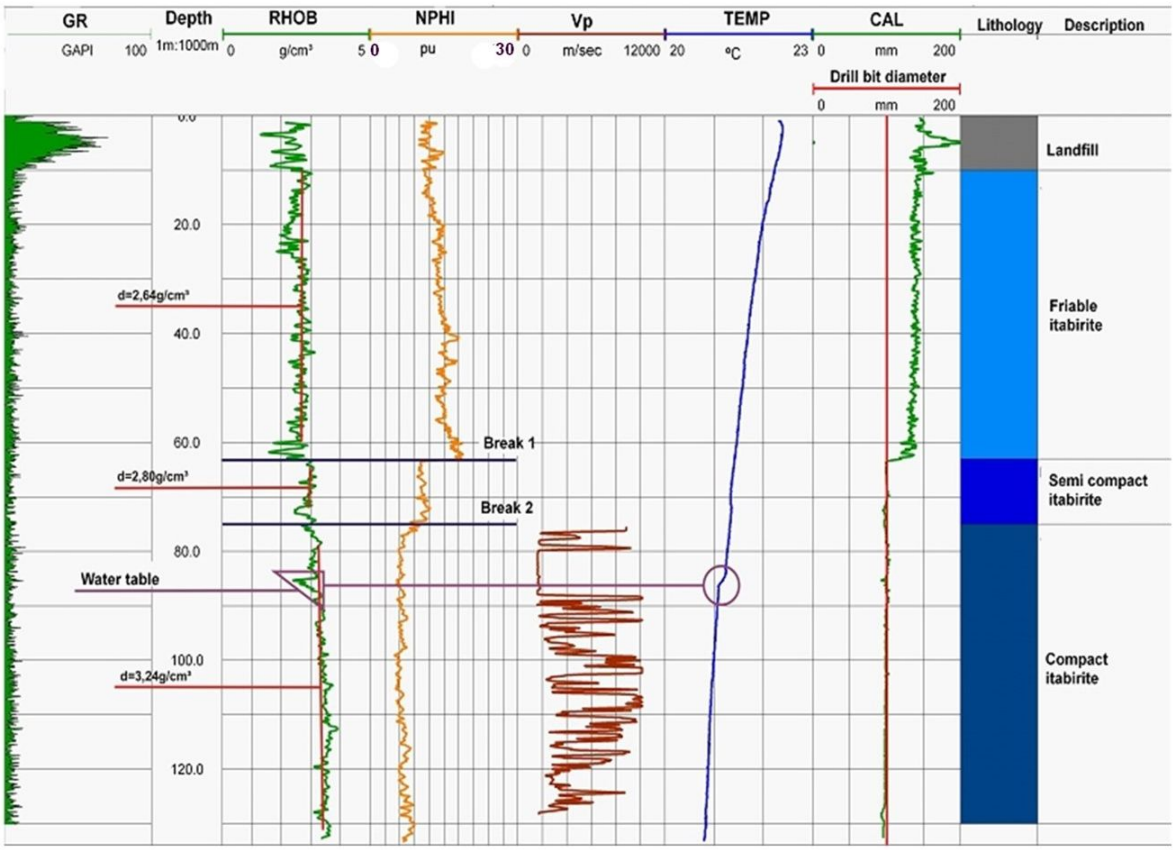

Figure 12: GR, RHOB, NPHI, Vp, TEMP and CAL, logs of the borehole FD-29, together with the lithology and its description. From 63.0 m depth, an increase in the RHOB log is recognized, showing reductions in the NPHI and CAL logs (Break 1). At 75.0 m, there is a new fall in the NPHI log and an increase in the RHOB log (Break 2). The inverted delta with little change in the CAL log at around 85.0 m was interpreted as the Water table, also observed in the TEMP log. The Vp shows an increase toward the bottom of the borehole, interpreted as a transition zone of itabirites with different degrees of compactness, friable up to 63.0 m, semi-compact and compact from 70.0 m to the end (Fonseca, 2014).

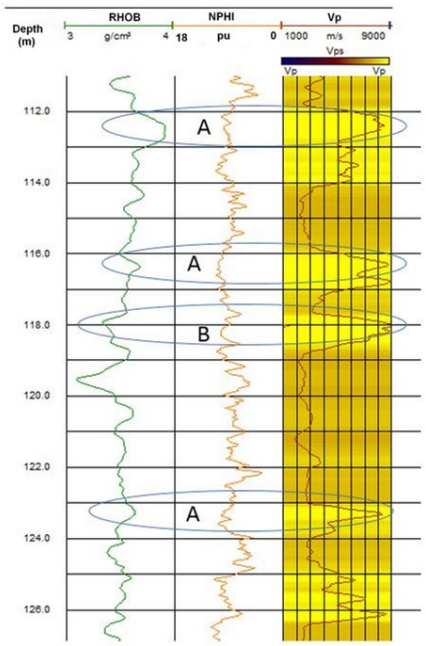

Figure 13: Details of RHOB, NPHI and V_p logs in the borehole FD-29 show (A) increased compactness, reduced porosity and increased density. (B) Increased compactness, reduced porosity, decreased density and increased V_p, probably because of the increased concentration of iron minerals (Fonseca, 2014).

due to the lack of soluble elements (red arrows in Figure 14), as seen in the GR, RHOB and NPHI logs. The PLO, identified as a clay layer with variable porosity and density in the GR, RHOB and NPHI logs, is designated for the 12.0 to 18.9 meters depth range. Smaller porosities may have altered the NPHI logs due to water in the pores or higher concentrations of hydrated minerals. The variations in the RHOB, NPHI and CAL logs indicate a more porous horizon with potential voids in the 18.9 -22.3 m depth range. The RHOB log does not show a grade from PLO to goethite hematite below 22.3 m. Nevertheless, the GR log shows a progressive drop in the clay concentration.

However, the CAL log reveals that the smaller diameters without asperities or breaking points are a more robust material (black arrow in Figure 14). On the other hand, variations in the V_p, NPHI, TEMP and CAL logs at 24.0 m depth are linked to a change in porosity and are taken to indicate the presence of the Water table (blue arrow in Figure 14). Below that, the GWL does not exhibit notable changes, moving to clayey levels with improved borehole wall stability. The RHOB log displays a "saw" pattern between 36.0 and 43.0 m, increasing from 2.5 to 2.9 g/cm3 because of an iron-richer interval (not shown). It then provides a drop that may indicate the change to the goethite itabirites described at 45.0 m. According to the geological description, a gray siliceous itabirite abruptly contacts another ocher and clay itabirite at 70.0 m.

The results of this study also point to potential changes in the drilling mesh, including a partial replacement of CS boreholes with rotary-percussive (RP) boreholes monitored with GWL. Considering a geological section with three drilled boreholes as an illustration, we can say that, in this situation, a central borehole with RP could be inserted with both CS ends serving as a guide for the geological interpretation. Figure 15 illustrates a drilling program for exploratory purposes in a specific and well-known geological setting, such as the Capanema Mine. From around 21 holes, 13 will be drilled with CS and 8 with RP, all having a GWL. An RP borehole generates an economy in relation to a CS borehole as it costs 35% less. A time consideration exists in addition to the cost reduction because a CS takes much longer to be completed than an RP borehole. The complexity of the geology and the level of detail needed for the project are two factors that affect all these changes.

CONCLUSIONS

To increase the use of geophysical well logs in mineral prospecting, the Brazilian mining company Vale S/A constructed a test site to calibrate these methods, especially the density log, whose measured property is significant for exploitation. Thus, three Capanema Mine boreholes were chosen to benefit from this initiative and advance this work. The study primary goal was to demonstrate the value of a joint interpretation of core sample data and logs in the delimitation of iron ores. The results show the importance of this method for locating the transition between friable and compact itabirites, defining lithological interfaces, detecting clay horizons, estimating the thickness of weathering layers and identifying hydrated materials. In general, the impact of increasing compression with depth on the density log measurements was more significant than the reduction in the content of heavy iron-rich minerals below 90 m depth during the analysis of itabirites. At this depth, the density log value changes from $2.80 to 3.24 gr/cm^3$ and the sonic log average value increases from 2000 to 7000 m/sec, indicating this fact. This study offers essential subsidies to improve methodologies applied for iron ores prospecting. It helps reduce research time and costs associated with mineral exploration when it is suggested to change the drilling mesh by substituting more rotary-percussive boreholes for core sample perforations, but always using geophysical well logs in both cases to support the geological interpretation of the subsurface.

ACKNOWLEDGMENTS

The authors thank the Brazilian mining company Vale S/A, the Federal University of Ouro Preto (UFOP), the National Council for Scientific and Technological Development (CNPq), the Laboratory of Engineering and Exploration of Petroleum (LENEP/UENF), the Geoactive Limited (Interactive Petrophysics software) and the National Institute of Science and Technology of Petroleum Geophysics (INCT-GP) for supporting this work.

REFERENCES

Cannon, S., 2016, Petrophysics: A practical guide: John Wiley & Sons, Ltd.

Darling, T., 2005, Well logging and formation evaluation: Gulf Professional Publishing.

Fonseca, L., 2014, Evaluation of geophysical logging methods in iron ore research – case study: Definition of lithologic contacts in mina capanema, mg: Master's thesis, Federal University of Ouro Preto (UFOP), School of Mines, Department of Geology, Ouro Preto, MG, Brazil. (Master's Thesis in Portuguese).

Franco, A., 2003, Geometry and tectonic evolution of the syncline ouro fino, iron quadrangle, mg: Master's thesis, Federal University of Ouro Preto (UFOP), School of Mines, Department of Geology, Ouro Preto, MG, Brazil. (Master's Thesis in Portuguese).

Guimarães, F., J. Massahud, and J. Viveiros, 1986, Capanema iron mine in the central part of the iron quadrangle, minas gerais, *in* Main Mineral Deposits of Brazil: DNPM / CVRD, **II**, 97–101. (in Portuguese).

Instituto de Pesquisas Tecnológicas (IPT), 2011, Technological control of concrete with different densities employed in executing gamma-gamma ray log calibration blocks: Technical report, Vale, Brazil. (Internal Report in Portuguese).

Kearey, P., M. Brooks, and I. Hill, 2002, An introduction

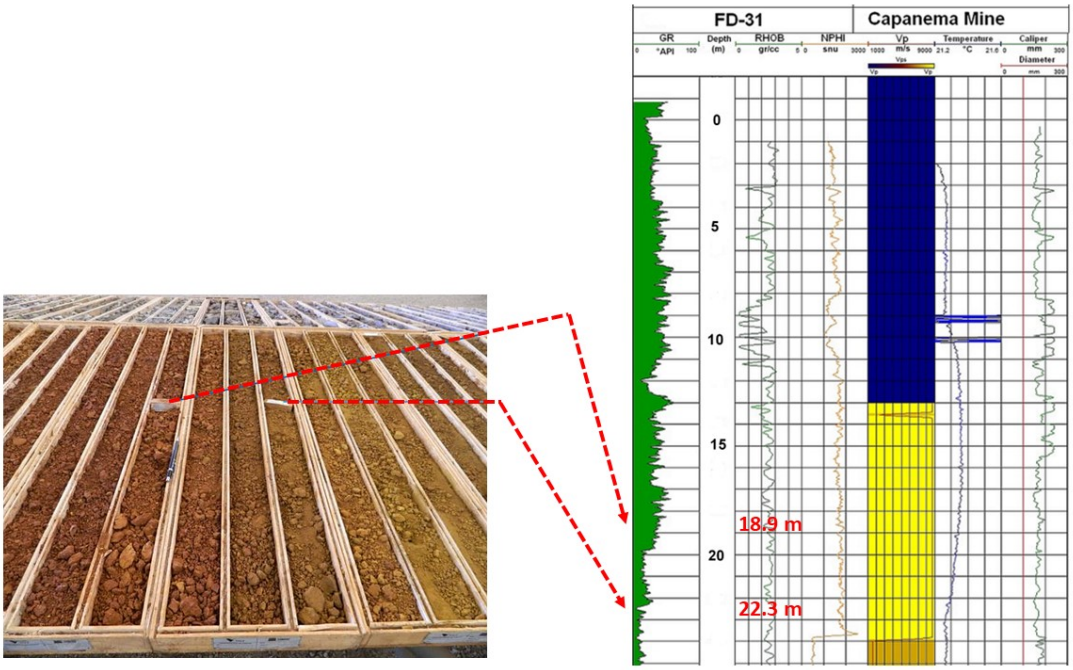

Figure 14: Borehole FD-31: (A) CS showing transitions between landfill to PLO (18.9 m) and PLO to yellow goethite hematite (22.3 m). (B) Well logs from left to right: GR, RHOB, NPHI, V_p, TEMP and CAL. The red arrows indicate the transition between landfill and PLO, the black arrow indicates the transition between PLO to goethite hematite, and the blue arrow indicates the water table (Fonseca, 2014).

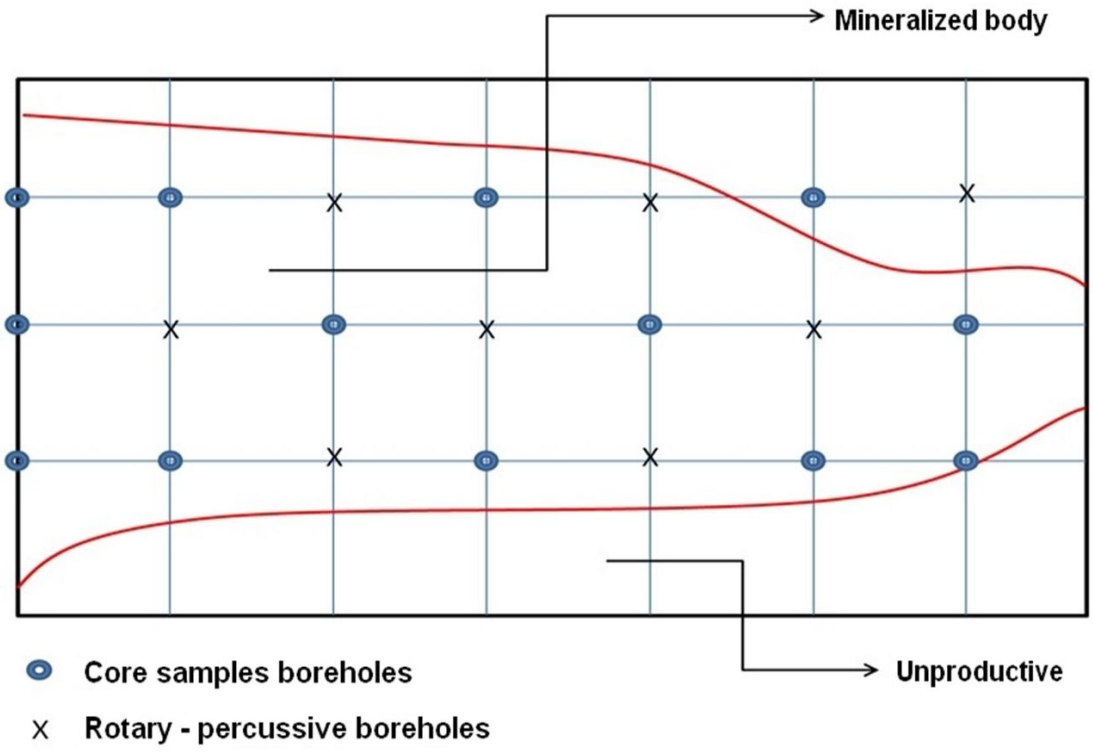

Figure 15: Programming of the hypothetical ore prospecting, showing the possibility of changing mesh drilling by replacing some CS with RP boreholes, using GWL to reduce time and costs in the survey (Fonseca, 2014).

to geophysical exploration, 3 ed.: Blackwell Science Ltd.

Lüthi, S., 2001, Geological well logs: Their use in reservoir modeling: Springer-Verlag.

MATLAB, 2014, Matlab User's Manual. MathWorks. (http://www.mathworks.com).

Oliveira, S., C. Uendro, G. Paranhos, R. Carmo, and M. Braga, 2011, Gamma-gamma ray geophysical logging as a tool to aid in the description and geological interpretation: 2nd Seminar of the Geology of Iron Ore and 1st of Speleology, VALE, 75. (in Portuguese).

Pena, N., 2013, Acoustic & optical televiewer: Technical report, Weatherford, Wireline Slimline Services. (Internal Report).

Rashidi, B., G. Hareland, and F. Shirkavand, 2009, Lithological determination from logs: Canadian International Petroleum Conference (CIPC), 8. doi: 10.2118/2009-180.

Rider, M., 2002, The geological interpretation of well logs: Whittles Publishing.

Schön, J., 2011, Physical properties of rocks: A workbook, volume **8** *of* Handbook of Petroleum Exploration and Production: Elsevier.

Spier, C., S. Oliveira, A. Sial, and F. Rios, 2007, Geochemistry and genesis of the banded iron formations of the Cauê Formation, Quadrilátero Ferrífero, Minas Gerais, Brazil: Precambrian Research, **152**, 170–206, doi: 10.1016/j.precamres.2006.10.003.

Vaz de Melo, M., and A. Seabra, 2000, Economic geology of the iron ore of são vicente mine, itabirito, mg: Technical report, Serra General Mining Company, Brazil. (Internal Report in Portuguese).

WellCad, 2014, Wellcad User's Manual. Advanced Logic Technology, Luxembourg.

Carrasquilla, A.G.: conceptualization, data interpretation, writing – original draft preparation, final figure edtion; **Fonseca, L.:** master's thesis development, data modeling.

Received on November 21, 2022 / Accepted on August 19, 2023